

## GaAs quantum structures: Comparison between direct pseudopotential and single-band truncated-crystal calculations

Alberto Franceschetti and Alex Zunger

Citation: *The Journal of Chemical Physics* **104**, 5572 (1996); doi: 10.1063/1.471797

View online: <http://dx.doi.org/10.1063/1.471797>

View Table of Contents: <http://scitation.aip.org/content/aip/journal/jcp/104/14?ver=pdfcov>

Published by the [AIP Publishing](#)

---

### Articles you may be interested in

[Modification of desorption phenomenon of Sb on Si surfaces by atomic hydrogen termination](#)

*Appl. Phys. Lett.* **69**, 1267 (1996); 10.1063/1.117387

[Effect of coupling between frustrated translation and libration on the nonthermal desorption of physisorbed CO: Three-dimensional quantum calculations](#)

*J. Chem. Phys.* **104**, 6330 (1996); 10.1063/1.471294

[Mechanism for the desorption of molecularly and dissociatively adsorbed methane on Pt\(111\) probed by pulse-laser heating](#)

*J. Chem. Phys.* **104**, 5974 (1996); 10.1063/1.471329

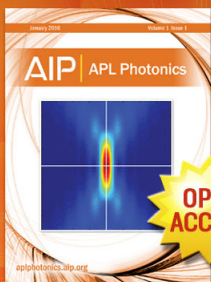
[Effects of adsorbate lateral repulsion on desorption and diffusion kinetics studied by Monte Carlo simulations](#)

*J. Chem. Phys.* **104**, 5674 (1996); 10.1063/1.471805

[Physisorbed surfaces studied by positron annihilation spectroscopy](#)

*AIP Conf. Proc.* **303**, 259 (1994); 10.1063/1.45501

---



Launching in 2016!

The future of applied photonics research is here

OPEN  
ACCESS

**AIP** | APL  
Photonics

# GaAs quantum structures: Comparison between direct pseudopotential and single-band truncated-crystal calculations

Alberto Franceschetti and Alex Zunger  
National Renewable Energy Laboratory, Golden, Colorado 80401

(Received 12 October 1995; accepted 3 January 1996)

A single-band approach for semiconductor clusters which accounts for the nonparabolicity of the energy bands was recently used by Rama Krishna and Friesner [M.V. Rama Krishna and R.A. Friesner, Phys. Rev. Lett. **67**, 629 (1991)]. We compare the results of this method (denoted here as single-band truncated-crystal, or SBTC, approximation) with a direct pseudopotential band-structure calculation for free-standing hydrogen-passivated GaAs quantum films, wires, and dots. The direct pseudopotential calculation, which includes coupling between all bands, shows that isolated GaAs quantum films, wires, and dots have an indirect band gap for thicknesses below 16, 28, and at least 30 Å (8, 14, and at least 15 ML), respectively; beyond these critical dimensions the transition becomes direct. A comparison of the SBTC approximation with the direct pseudopotential calculation shows that (i) the confinement energy of the valence-band maximum is overestimated by the SBTC method, because the zero-confinement character of this state is neglected; (ii) the confinement energy of the  $\Gamma$ -derived conduction state (direct band gap) is slightly overestimated by the SBTC approximation, mainly because of the assumption of infinite potential barriers at the boundaries; (iii) the confinement energy of the  $X$ -derived conduction state (indirect band gap) is severely underestimated by the SBTC method; (iv) while the SBTC approximation predicts “quantum deconfinement” (i.e., reduction of gap as size is reduced) for the direct gap of thin GaAs quantum wires, such effect is not present in the direct pseudopotential calculation. © 1996 American Institute of Physics. [S0021-9606(96)00114-7]

## I. INTRODUCTION

The one-band effective-mass approximation (EMA) has been widely used to predict optical and electronic properties of semiconductor nanostructures.<sup>1</sup> In the case of semiconductor clusters embedded in organic solvents or colloidal suspensions, however, the agreement of the calculated band gap with experiment turns out to be rather poor, especially for small cluster sizes.<sup>2</sup> This disagreement can be traced back to the fact that the EMA neglects (i) the nonparabolic energy dispersion of the band-edge states, and (ii) the coupling between different bulk states introduced by the lack of translational invariance.

To account for nonparabolicity effects within a single-band approach, Rama Krishna and Friesner<sup>3-5</sup> have recently used a band structure formalism, denoted here as single-band truncated-crystal (SBTC) approximation, in which the cluster energy levels are represented by those of an extended, periodic bulk solid, evaluated at special wave vectors  $\mathbf{k}^*$  satisfying the particle-in-a-box quantization rules. The mapping of the cluster energy levels onto the bulk band structure was first proposed in the 1970's (Refs. 6 and 7) in the tight-binding context. The novelty of the method proposed by Rama Krishna and Friesner consists of the use of empirical pseudopotentials to calculate the bulk band structure. A comparison between SBTC and EMA results for the direct band gap of GaAs spherical clusters (Fig. 1) demonstrates that (i) the EMA band gap is overestimated with respect to the SBTC band gap, and (ii) a remarkable feature of the SBTC results, i.e. the existence of “quantum deconfinement” (re-

duction of gap as size is reduced) for small cluster sizes,<sup>8</sup> is absent in the EMA description.

While the SBTC method is relatively straightforward and computationally fast, the physical justification for the underlying single-band approximation is unclear, at least in the case of quantum wires and dots. In fact, while it has been shown<sup>8</sup> that in a two-dimensional (2D) quantum film the one-dimensional zero boundary conditions (vanishing wave function at  $z=0$  and  $z=L$ ) can be approximately satisfied by expanding the film wave function in terms of bulk wave functions belonging to the same bulk band, this has never been proved for quantum wires or quantum dots, where one needs to match boundary conditions in two and three dimensions, respectively. Thus, although the single-band approximation becomes exact in the limit of very large clusters, interband coupling is expected to play a significant role in nanometer-size clusters.

A previous pseudopotential calculation for indirect-gap Si clusters<sup>9</sup> showed that the SBTC approximation severely *underestimates* the band gap,<sup>10</sup> e.g., by as much as  $\sim 1$  eV for a diameter of 15 Å. We report here on a systematic comparison of the SBTC approximation with a direct pseudopotential calculation for GaAs quantum films, wires, and dots (denoted in the following as quantum structures). We find that (i) the confinement energy of the valence-band maximum (VBM) is *overestimated* by the SBTC method, because of the zero-confinement character of this state; (ii) the confinement energy of the  $\Gamma$ -derived conduction-band minimum (CBM) is slightly *overestimated* by the SBTC approxima-

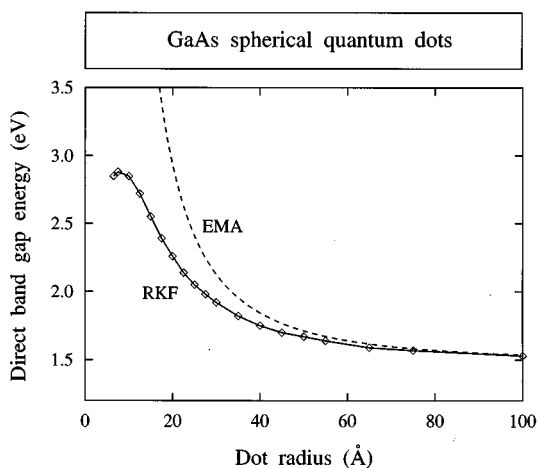


FIG. 1. Energy of the *direct* band gap of GaAs spherical quantum dots as a function of the dot radius, as published by Rama Krishna and Friesner (Ref. 4) (solid line) and according to a standard effective-mass calculation with infinite potential barriers (dashed line). The exciton binding energy is omitted in both cases.

tion, mainly because of the assumption of infinite potential barriers at the boundaries; (iii) the confinement energy of the  $X$ -derived conduction state (indirect gap) is severely *underestimated* by SBTC; (iv) while the SBTC approximation predicts quantum deconfinement for the direct gap of thin GaAs quantum wires, such effect is not present in the direct pseudopotential calculation, and is therefore an artifact of the SBTC approximation.

## II. METHODS

### A. Direct diagonalization

In the direct diagonalization (DD) approach we solve for the single-particle Schrödinger equation (in atomic units):

$$[-1/2\nabla^2 + V_{\text{QS}}(\mathbf{r})]\psi_i(\mathbf{r}) = \epsilon_i\psi_i(\mathbf{r}), \quad (1)$$

where  $V_{\text{QS}}(\mathbf{r})$  is the total pseudopotential of the quantum structure.  $V_{\text{QS}}$  is described here by the sum of screened atomic pseudopotentials centered at the atomic positions  $\mathbf{R}_n$ :

$$V_{\text{QS}}(\mathbf{r}) = \sum_n v_n(\mathbf{r} - \mathbf{R}_n). \quad (2)$$

For Ga and As atoms we use the nonrelativistic atomic pseudopotentials developed by Mäder and Zunger.<sup>11</sup> Using a plane-wave basis set with an energy cutoff  $E_{\text{cut}} = 5$  Ry, these pseudopotentials are carefully fitted to measured interband transition energies and effective masses of bulk GaAs, and to the work function of the (110) surface. In particular, the calculated direct band gap ( $\Gamma_{15v} - \Gamma_{1c}$  transition) is 1.52 eV, while the energies of the indirect  $\Gamma_{15v} - X_{1c}$  and  $\Gamma_{15v} - L_{1c}$  transitions are 2.00 and 1.81 eV, respectively. The dangling bonds at the surface of the quantum structure are passivated using hydrogenic pseudopotentials. In the case of (110) and  $(\bar{1}\bar{1}0)$  surfaces, each Ga or As atom has only one dangling

bond, which is passivated by a hydrogen atom located along the direction of the dangling bond itself. In the case of the (001) surface (which we assume to be As terminated), each As atom has two dangling bonds, which are passivated by a pair of hydrogen atoms. To avoid interaction between the hydrogen atoms located along the  $[1\bar{1}0]$  chains, we tilt each pair of hydrogen atoms around the  $[\bar{1}\bar{1}0]$  axis. The effect of this hydrogen-like potential is to remove the surface states from the band gap and to decouple the band-edge states from surfacelike states.

Since the quantum structures considered here contain hundreds, or even thousands, of atoms per unit cell, conventional diagonalization techniques are not practical for solving the eigenvalue problem. Instead, the band-edge states of the quantum structures are obtained using the folded spectrum method,<sup>12</sup> which searches for the ground state of the operator  $(\hat{H} - \epsilon_{\text{ref}})^2$ , where  $\hat{H} = -1/2\nabla^2 + V_{\text{QS}}$  is the pseudo-Hamiltonian of the quantum structure and  $\epsilon_{\text{ref}}$  is an arbitrary reference energy. The ground state of this operator is the eigenstate of  $\hat{H}$  closest in energy to the reference level  $\epsilon_{\text{ref}}$ ; by choosing  $\epsilon_{\text{ref}}$  in the band gap, one obtains the band-edge states of the quantum structure, with the same accuracy achieved in a conventional diagonalization of the Hamiltonian.

The hydrogen-passivated GaAs quantum structure is embedded in vacuum, and the quantum structure + vacuum “supercell” is repeated periodically. The size of the vacuum region is increased until the effect of the spurious interaction between quantum structures on the energy levels becomes negligible. Using (artificial) periodic boundary conditions, the quantum structure wave function can be conveniently expanded in a plane wave basis set:

$$\psi(\mathbf{r}) = \sum_{\mathbf{G}} c(\mathbf{G})e^{i\mathbf{G}\cdot\mathbf{r}}, \quad (3)$$

where the sum runs over the reciprocal lattice vectors of the supercell. The same energy cutoff ( $E_{\text{cut}} = 5$  Ry) used in Ref. 11 to generate the atomic pseudopotentials is adopted in the supercell calculation, in order to assure consistent band gaps in the limit of large quantum structures. The functional  $\langle \psi | (\hat{H} - \epsilon_{\text{ref}})^2 | \psi \rangle$  is minimized with respect to the coefficients  $c(\mathbf{G})$  using a preconditioned conjugate-gradients algorithm. The matrix-by-vector product  $(\hat{H} - \epsilon_{\text{ref}})|\psi\rangle$ , which occurs in the calculation of the conjugate gradients, is efficiently performed using a double-space formalism: the kinetic energy part is calculated in reciprocal space, where the kinetic energy operator is diagonal, while the potential energy part is calculated in real space, where the potential energy operator is diagonal. Optimized fast Fourier transforms are used to switch from reciprocal space to real space and vice versa. Since only the band-edge states are explicitly calculated, the overall computational effort scales as  $O(N \log N)$ , where  $N$  is the number of atoms, as opposed to the  $N^3$  scaling of conventional diagonalization techniques.

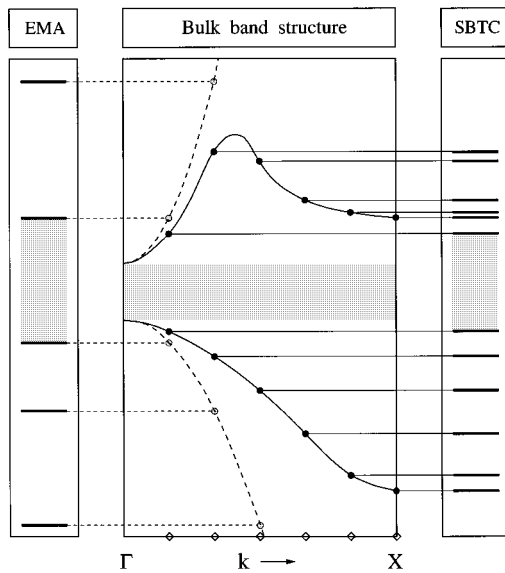


FIG. 2. Schematic illustration of the conventional EMA (left column) and of the SBTC approximation (right column) for a 2D quantum film. The solid lines in the central part of the figure represent the bulk band structure in the direction perpendicular to the film orientation. According to the SBTC approximation, the film energy levels at the zone center are extracted from the bulk band structure calculated at selected  $\mathbf{k}^*$  wave vectors, denoted by diamond shapes on the abscissa. In the EMA, the film energy levels are obtained with the additional approximation of parabolic bulk bands (dashed lines). The shaded areas denote the forbidden gaps. Note that because of the parabolic approximation the band gap is larger in the EMA than in the SBTC approximation. The SBTC approximation is superior to the EMA as no parabolicity of the dispersion relation is assumed.

## B. Single-band truncated-crystal approximation

The same Ga and As atomic pseudopotentials used in the direct minimization procedure are applied to the calculation of the bulk band structure, in order to extract the quantum structure energy levels according to the SBTC scheme. Denoting by  $\epsilon_n^{\text{bulk}}(\mathbf{k})$  the energy dispersion<sup>13</sup> of the bulk band  $n$ , in the SBTC approximation one introduces an effective Hamiltonian  $H_n^{\text{SBTC}}$  by replacing the wave vector  $\mathbf{k}$  with the operator  $-i\nabla$ :

$$H_n^{\text{SBTC}} = \epsilon_n^{\text{bulk}}(-i\nabla). \quad (4)$$

Note that the SBTC Hamiltonian reduces to the conventional effective-mass Hamiltonian when  $\epsilon_n^{\text{bulk}}(\mathbf{k})$  is parabolic. Thus, the non-parabolicity of the energy bands is fully included in the SBTC approximation. The Schrödinger equation for the SBTC Hamiltonian is solved assuming zero boundary conditions at the surface of the quantum structure. Therefore, the *eigenfunctions* of the SBTC hamiltonian coincide with the effective-mass envelope functions satisfying the same boundary conditions. The *eigenvalues* of the SBTC Hamiltonian, on the other hand, are given by the bulk energy levels calculated at selected  $\mathbf{k}^*$  points in the first Brillouin zone satisfying the particle-in-a-box quantization rules. For example, in the case of a rectangular quantum box of size  $L_1, L_2, L_3$  one has  $\mathbf{k}^* = \pi(n_1/L_1, n_2/L_2, n_3/L_3)$ , where  $n_1, n_2, n_3$  are nonzero integer quantum numbers.

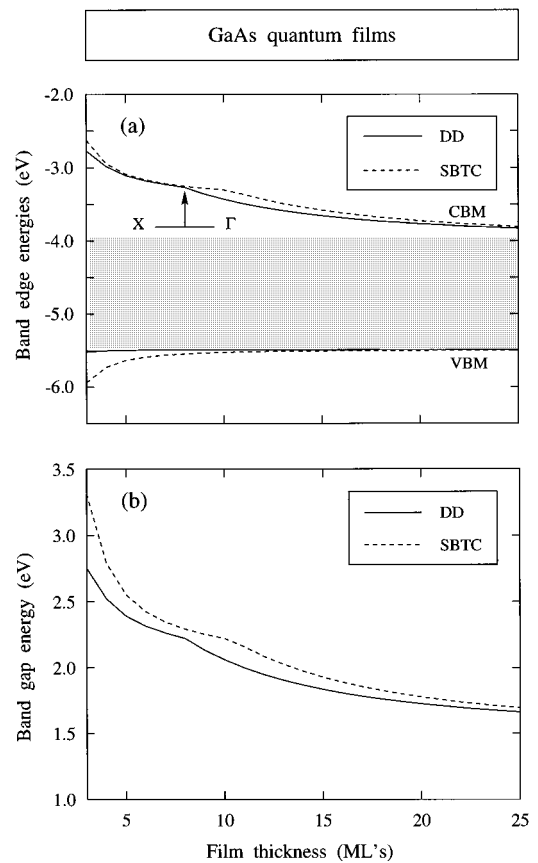


FIG. 3. (a) Band-edge energies and (b) band-gap energy of free-standing, hydrogen-passivated GaAs (110) quantum films as a function of the film thickness (in ML's), according to a direct pseudopotential calculation (solid lines) and to the SBTC approximation (dashed lines). The bulk band gap is denoted by the shaded area in part (a). The vertical arrow indicates the  $X \rightarrow \Gamma$  crossover of the conduction-band minimum.

The SBTC method is schematically illustrated in Fig. 2, together with the conventional EMA, for a 2D quantum film. Two steps are involved in the practical implementation of the SBTC approximation: (i) a set of wave vectors  $\mathbf{k}^*$  is selected according to the particle-in-a-box quantization conditions; (ii) the energy levels of the quantum structure are approximated by the eigenvalues of the bulk solid calculated at these selected  $\mathbf{k}^*$  points. Note that in the SBTC method, as well as in the EMA, the zone center  $\Gamma$  point is always excluded from the set of  $\mathbf{k}^*$  points, thus providing an explanation for the band-gap increase in quantum structures relative to the bulk (see Fig. 2).

## III. RESULTS AND DISCUSSION

We will consider free-standing, isolated GaAs quantum films (2D), quantum wires (1D), and quantum dots (0D), comparing the results of the SBTC approximation to those obtained by direct diagonalization.

### A. Quantum films

We start by considering a case where the single-band approximation is known<sup>6,8</sup> to work well, namely a 2D free-

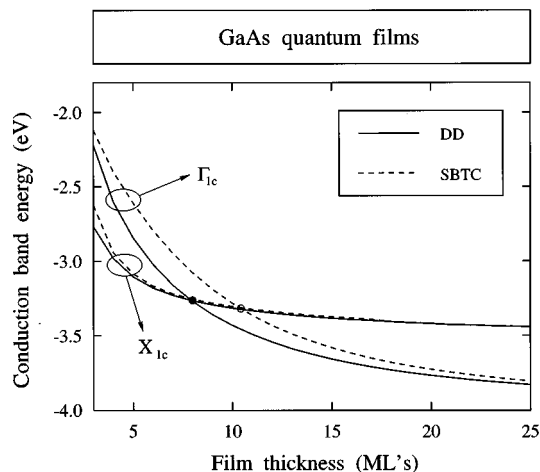


FIG. 4. Energy of the  $X$ -derived and  $\Gamma$ -derived conduction states of GaAs quantum films. The critical size for the occurrence of the  $X \rightarrow \Gamma$  transition, as obtained from the direct diagonalization and from the SBTC approximation, is denoted by a solid circle and a dashed circle, respectively.

standing GaAs quantum film oriented in the  $(1\bar{1}0)$  plane. The set of  $\mathbf{k}^*$  points satisfying the particle-in-a-box quantization rule is given by

$$\mathbf{k}_l^* = \pi/\sqrt{2}L (l, -l, 0), \quad (5)$$

where  $L$  is the film thickness and  $l$  is a nonzero integer. According to the SBTC method, the film eigenvalues  $\epsilon_i^{\text{film}}$  are approximated by the bulk band energies calculated at these  $\mathbf{k}^*$  points.

The band-edge energies at the zone center of the two-dimensional Brillouin zone, calculated with the SBTC approximation and with the direct pseudopotential approach, are compared in Fig. 3(a) as a function of the film thickness  $L$  (note that in the  $\langle 110 \rangle$  directions 1 GaAs ML  $\approx 2.0 \text{ \AA}$ ). In the “exact” pseudopotential calculation the VBM of the quantum film is a zero-confinement state,<sup>8,14</sup> whose energy is almost independent of the film thickness  $L$ . The conduction-band minimum originates from the  $X_{1c}$  valley for  $L < 8$  ML’s, while it becomes a  $\Gamma_{1c}$  derived state for  $L > 8$  ML’s; the  $X \rightarrow \Gamma$  crossover is evident in Fig. 3(a) from the change of slope of the energy vs thickness curve. The SBTC approximation gives a good overall description of the near-edge states of GaAs quantum films, but fails to describe the zero-confinement nature of the VBM, and slightly overestimates the CBM confinement energy. Figure 3(b) shows the band gap as a function of  $L$ . The SBTC band gap is overestimated typically by  $\sim 0.2$  eV for  $L < 15$  ML’s.

The  $X$ -derived and  $\Gamma$ -derived conduction-band energies are shown in more detail in Fig. 4 as a function of the film thickness  $L$ . We see that the SBTC error in energy is larger for the  $\Gamma$ -derived state than for the  $X$ -derived state. The  $X \rightarrow \Gamma$  crossover is clearly visible in this figure; it is predicted to occur at  $L \sim 8$  ML’s by the direct diagonalization method ( $L \sim 13$  ML’s for a GaAs/AlAs quantum well<sup>15</sup>), and at  $L \sim 10$  ML’s by the SBTC approximation (see also Table I). Note that for 2D quantum films (both in the “exact”

TABLE I. Critical sizes (in ML’s) for the  $X \rightarrow \Gamma$  crossover in GaAs quantum films, wires, and dots, according to the direct pseudopotential calculation (DD) and to the single-band truncated-crystal approximation (SBTC).

|      | DD     | SBTC   |
|------|--------|--------|
| Film | 8      | 10     |
| Wire | 14     | 20     |
| Dot  | $> 15$ | $> 15$ |

pseudopotential results and in the SBTC approximation) there is no quantum deconfinement in either the  $\Gamma$ -derived state or the  $X$ -derived state: the energy of these states increases monotonically as the film thickness decreases.

## B. Quantum wires

We now consider GaAs quantum wires with square cross section; the surface planes are oriented in the  $(1\bar{1}0)$  and  $(110)$  directions, and the wires are periodic in the  $[001]$  direction. The  $\mathbf{k}^*$  points satisfying the particle-in-a-box quantization rules are

$$\mathbf{k}_{l,m}^* = \pi/\sqrt{2}L (l+m, l-m, 0), \quad (6)$$

where  $L$  is the wire thickness in the  $[1\bar{1}0]$  and  $[110]$  directions and  $l, m$  are nonvanishing integers.

The band-edge energies at the zone center of the one-dimensional Brillouin zone, obtained using the direct diagonalization approach and the SBTC approximation, are compared in Fig. 5(a) as a function of the wire size  $L$ . The VBM confinement energy is overestimated by the SBTC method, because the wave function retains a zero-confinement component. Furthermore, the CBM energy is significantly underestimated by the SBTC approximation. For  $L < 14$  ML’s the CBM wave function derives from the  $X_{1c}$  valley; for wider wires the CBM becomes a  $\Gamma_{1c}$ -derived state, according to the direct pseudopotential calculation. The SBTC method, on the other hand, predicts the CBM to be  $X$ -like up to  $L \sim 20$  ML’s (see also Table I). The SBTC band gap [Fig. 5(b)] turns out to be in relatively good agreement with the direct diagonalization, *because the errors in the VBM and CBM energies [Fig. 5(a)] tend to cancel*.

The energies of the  $X$ -derived and  $\Gamma$ -derived conduction-band states are shown in more detail in Fig. 6 as a function of the wire thickness  $L$ . According to the SBTC approximation, the energy of the direct ( $\Gamma$ -derived) conduction-band state shows a turnaround at  $L \sim 7$  ML’s (deconfinement effect). This effect is not present in the direct pseudopotential calculation. While the extent of the deconfinement effect depends on the details of the pseudopotential, our calculations demonstrate that in this case the turnaround is an artifact of the SBTC approximation.

The  $X \rightarrow \Gamma$  crossover of the CBM, which occurs at  $L \sim 14$  ML’s according to the direct pseudopotential calculation, is illustrated in Fig. 7, where the CBM wave function

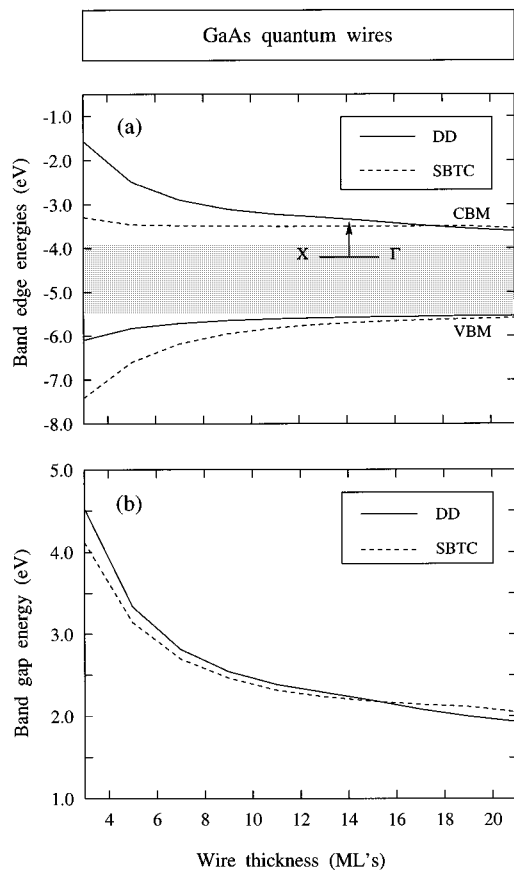


FIG. 5. (a) Band-edge energies and (b) band-gap energy of free-standing GaAs  $(\bar{1}\bar{1}0) \times (110)$  quantum wires as a function of the wire thickness (in ML's), according to a direct pseudopotential calculation (solid lines) and to the SBTC approximation (dashed lines). The bulk band gap is indicated by the shaded area in part (a). The vertical arrow indicates the  $X \rightarrow \Gamma$  crossover of the conduction-band minimum.

amplitude is plotted in the  $(\bar{1}\bar{1}0) \times (110)$  plane for  $L = 13$  ML's and  $L = 15$  ML's. The change of symmetry of the CBM wave function is evident in Fig. 7.

### C. Quantum dots

We finally consider GaAs quantum boxes with rectangular shape, elongated in the  $[001]$  direction. The surface planes are oriented in the  $(\bar{1}\bar{1}0)$ ,  $(110)$ , and  $(001)$  directions. We have  $L_{1\bar{1}0} = L_{110} = L$  and  $L_{001} = \sqrt{2}L$ , and the  $\mathbf{k}^*$  points are given by

$$\mathbf{k}_{l,m,n}^* = \pi/\sqrt{2}L (l+m, l-m, n), \quad (7)$$

where  $l, m, n$  are nonvanishing integers.

The band-edge energies obtained using the SBTC approximation and the direct pseudopotential approach are compared in Fig. 8(a) as a function of the dot size  $L$ . The complete pseudopotential calculation predicts an indirect ( $X$ -derived) conduction-band minimum in all the size range considered here. As the size increases, however, the CBM will eventually become a direct,  $\Gamma$ -derived state. As in the case of quantum wires, we see that the VBM confinement

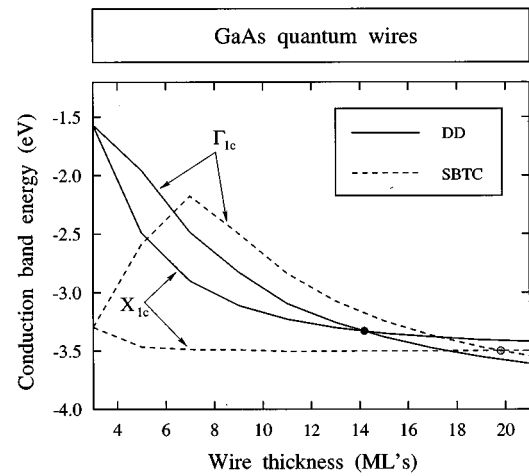


FIG. 6. Energy of the  $X$ -derived and  $\Gamma$ -derived conduction states of free-standing GaAs quantum wires. The critical size for the occurrence of the  $X \rightarrow \Gamma$  transition, as obtained from the direct diagonalization and from the SBTC approximation, is denoted by a solid circle and a dashed circle, respectively. Note the absence of quantum deconfinement in the direct pseudopotential calculation.

energy is overestimated by SBTC, while the CBM confinement energy is significantly underestimated. Because of this cancellation, however, the SBTC gap [Fig. 8(b)] is in good agreement (at least for  $L \geq 5$  ML's) with the direct pseudopotential calculation.

## IV. IMPROVING THE SBTC APPROXIMATION

### A. Extended SBTC approximation

The GaAs quantum structures considered here have an *indirect* ( $X_{1c}$ -derived) CBM at small sizes, because the light-mass  $\Gamma_{1c}$ -like state is pushed up by quantum-confinement effects faster than the heavier-mass  $X_{1c}$ -like state. The SBTC approximation severely *underestimates* the confinement energy of the  $X$ -derived CBM of small quantum wires and dots [Figs. 5(a) and 8(a)]. This is a consequence of the fact that

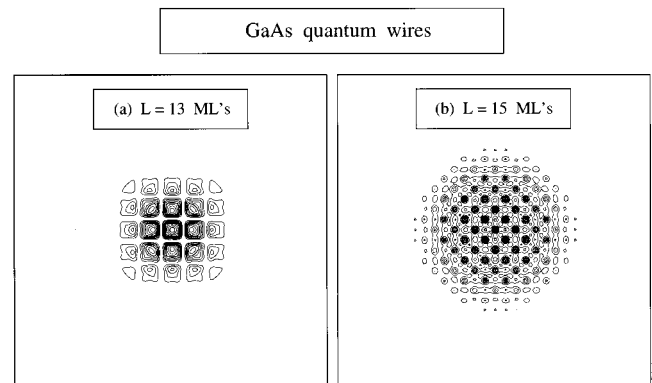


FIG. 7. CBM wave function of free-standing GaAs quantum wires. The wave function amplitude, averaged along the wire direction, is plotted in the  $(\bar{1}\bar{1}0) \times (110)$  plane. Note the change of symmetry in going from (a)  $L = 13$  ML's to (b)  $L = 15$  ML's.

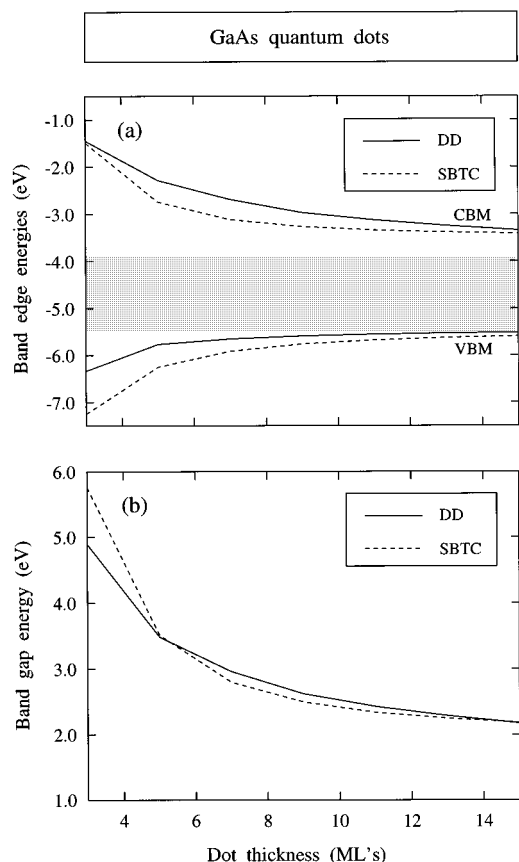


FIG. 8. (a) Band-edge energies and (b) band-gap energy of free-standing GaAs  $(110) \times (1\bar{1}0) \times (001)$  quantum boxes as a function of the box thickness (in ML's), according to a direct pseudopotential calculation (solid lines) and to the SBTC approximation (dashed lines). The bulk band gap is indicated by the shaded area in part (a). The band gap of the quantum box differs from the one shown in Fig. 1 (taken from Ref. 4), because only the *direct* ( $\Gamma$ -derived) band gap is shown there.

the SBTC method picks up only *one* (or a few, if degenerate)  $\mathbf{k}^*$  point(s) in the Brillouin zone as the CBM wave vector(s); in general, this approximation is insufficient to satisfy zero boundary conditions in quantum wires and dots. This error can be partially corrected by introducing an “extended” single-band truncated-crystal (E-SBTC) approximation, where each conduction-band valley is treated independently from the others. This method was first discussed by Zhang, Yeh and Zunger<sup>8</sup> in the case of Si quantum films. Denoting by  $\mathbf{k}_0$  the wave vector of a particular valley<sup>16</sup> (e.g.,  $\Gamma_{1c}$ ,  $X_{1c}^x$ ,  $X_{1c}^y$ ,  $X_{1c}^z$ , etc.), in the E-SBTC approximation we (i) apply the particle-in-a-box quantization rules to the  $(\mathbf{k}-\mathbf{k}_0)$  wave vector; (ii) calculate the quantized wave vectors  $\mathbf{k}^*$  corresponding to the lowest allowed particle-in-a-box indexes [e.g.,  $\mathbf{k}^* = \mathbf{k}_0 + \pi(\pm 1/L_1, \pm 1/L_2, \pm 1/L_3)$  in the case of a rectangular quantum box]; (iii) average over the bulk band energies calculated at these  $\mathbf{k}^*$  points (which are, in general, nondegenerate). The results of this approach, including the  $X_{1c}$  and  $\Gamma_{1c}$  conduction-band valleys, are shown in Fig. 9(a) for quantum wires and in Fig. 9(b) for quantum dots (dotted lines). Except for the extreme limit  $L=3$  ML's, the agreement with the direct diagonalization results is

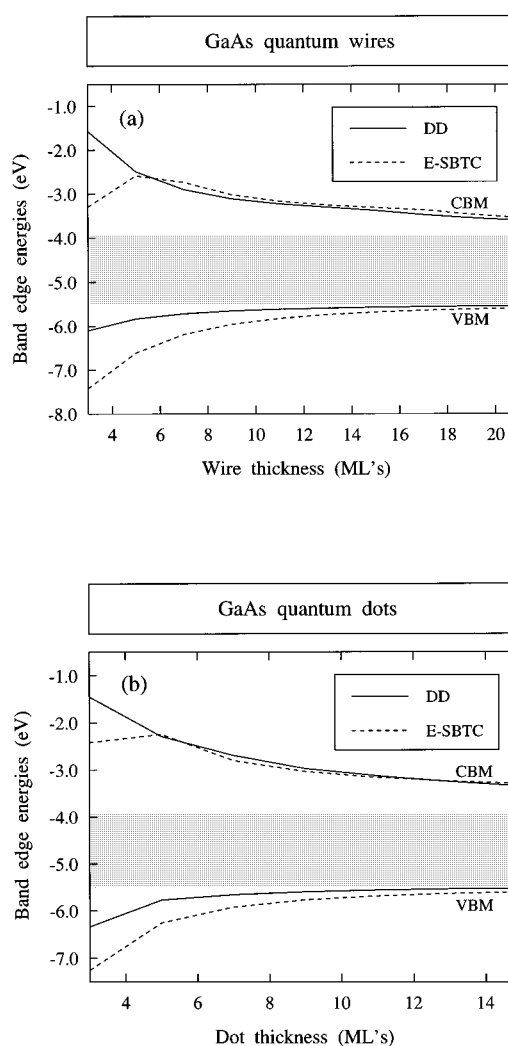


FIG. 9. Band-edge energies of (a) GaAs quantum wires and (b) GaAs quantum dots, according to the direct pseudopotential calculation (solid lines) and to the E-SBTC approximation (dashed lines).

greatly improved over the SBTC method, and the error is comparable to the case of quantum films. Note that in the case of  $(1\bar{1}0)$  quantum films (where only points along the  $\Gamma - X^z$  line fold into the zone center) the SBTC and E-SBTC approximations give identical results for the zone-center band gap.

## B. Finite-well SBTC approximation

In the standard SBTC approximation the set of particle-in-a-box  $\mathbf{k}^*$  wave vectors is obtained assuming zero boundary conditions, corresponding to an infinite potential barrier outside the quantum structure. In reality, however, the potential barrier is finite, and it is related to the work function of the quantum structure. In the finite-well single-band truncated-crystal (FW-SBTC) approximation the finite potential well is taken into account in the quantization of the  $\mathbf{k}^*$  wave vectors. For example, in the case of  $(110)$  quantum films Eq. (5) is replaced, for each valley  $\mathbf{k}_0$ , by

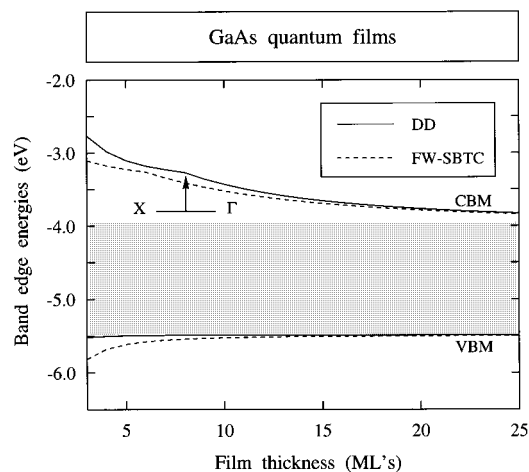


FIG. 10. Band-edge energies of GaAs ( $\bar{1}\bar{1}0$ ) quantum films as a function of the film thickness, as obtained from the direct pseudopotential calculation (solid line) and from the FW-SBTC approximation (dashed line).

$$\mathbf{k}^* = \mathbf{k}_0 \pm \eta / \sqrt{2} (1, -1, 0), \quad (8)$$

where  $\eta$  is the smallest nonvanishing solution of the implicit equation

$$\tan\left(\frac{L}{\eta}\right) = \frac{(2m_0^*V_0 - \eta^2)^{1/2}}{\eta}. \quad (9)$$

Here  $m_0^*$  is the effective mass of the valley  $\mathbf{k}_0$  in the  $[\bar{1}\bar{1}0]$  direction, and  $V_0$  is the finite potential barrier (in atomic units). The former is obtained directly from our pseudopotential calculation for bulk GaAs, while the latter is obtained as the difference between the work function and the energy of the bulk  $\mathbf{k}_0$  valley, calculated with respect to the VBM. Note that if  $V_0 \rightarrow \infty$  from Eq. (9) we obtain  $\eta \rightarrow \pi/L$ , and the FW-SBTC approximation reduces to the E-SBTC approximation.

The FW-SBTC approximation is illustrated in Fig. 10 in the case of GaAs ( $\bar{1}\bar{1}0$ ) quantum films. The agreement with the “exact” pseudopotential results is slightly improved with respect to the standard SBTC approximation [compare with Fig. 3(a)], especially for  $L > 8$  ML's. However, the FW-

SBTC tends to overcorrect the error in the confinement energy of the CBM, which is now slightly underestimated.

## ACKNOWLEDGMENTS

The authors are grateful to Professor Rama Krishna for useful comments and suggestions. This work was supported by the U.S. Department of Energy, OER-BES, under Grant No. DE-AC36-83CH10093.

<sup>1</sup>L. Brus, IEEE J. Quantum Electron., **QE-22** **9**, 1909 (1986); M.G. Bawendi, M.L. Steigerwald, and L.E. Brus, Annu. Rev. Phys. Chem. **41**, 477 (1990); U. Woggon and S.V. Gaponenko, Phys. Status Solidi B **189**, 285 (1995).

<sup>2</sup>See, for example, A.D. Yoffe, Adv. Phys. **42**, 173 (1993).

<sup>3</sup>M.V. Rama Krishna and R.A. Friesner, Phys. Rev. Lett. **67**, 629 (1991).

<sup>4</sup>M.V. Rama Krishna and R.A. Friesner, J. Chem. Phys. **95**, 8309 (1991).

<sup>5</sup>A. Tomasulo and M.V. Rama Krishna (unpublished).

<sup>6</sup>A. Zunger, J. Phys. C **7**, 96 (1974).

<sup>7</sup>O. Bilek and L. Skala, Czech. J. Phys. B **28**, 1003 (1978); P. Kadura and L. Künne, Phys. Status Solidi B **88**, 537 (1978); L. Künne, L. Skala, and O. Bilek, Czech. J. Phys. B **29**, 1030 (1979); O. Bilek, L. Skala, and L. Künne, Phys. Status Solidi B **117**, 675 (1983); L. Künne, L. Skala, and O. Bilek, *ibid.* **118**, 173 (1983).

<sup>8</sup>S.B. Zhang and A. Zunger, Appl. Phys. Lett. **63**, 1399 (1993); S.B. Zhang, C.-Y. Yeh, and A. Zunger, Phys. Rev. B **48**, 11204 (1993); C.-Y. Yeh, S.B. Zhang, and A. Zunger, *ibid.* **50**, 14405 (1994).

<sup>9</sup>L.W. Wang and A. Zunger, in *Nanocrystalline Semiconductor Materials*, edited by P.V. Kamat and D. Meisel (Elsevier, New York, in press).

<sup>10</sup>The results of Rama Krishna and Friesner agree with experimental photoluminescence data, that involves, most likely, gap states. The absorption threshold energy, however, is higher than the photoluminescence energy (although lower than the direct band gap of Silicon); see, for example, D.J. Lockwood, Solid State Commun. **92**, 101 (1994); D.J. Lockwood and A.G. Wang, *ibid.* **94**, 905 (1995). The results of the direct pseudopotential calculation of Ref. 9 agree very well with this absorption data.

<sup>11</sup>K.A. Mäder and A. Zunger, Phys. Rev. B **50**, 17393 (1994).

<sup>12</sup>L.W. Wang and A. Zunger, J. Chem. Phys. **100**, 2394 (1994); J. Phys. Chem. **98**, 2158 (1994).

<sup>13</sup>We make the assumption here that the energy dispersion  $\epsilon_n^{\text{bulk}}(\mathbf{k})$  of the bulk band  $n$  can be described by an analytic function of  $k_x^2$ ,  $k_y^2$ , and  $k_z^2$ . This is always true for the zinc-blende structure.

<sup>14</sup>The zero-confinement character of the valence-band maximum is a property of free-standing 2D quantum films, where the VBM wave function is required to vanish at the boundaries. When a film is embedded in a barrier semiconductor, e.g., GaAs in AlGaAs, no zero-confinement state occurs. See, for example, A. Franceschetti and A. Zunger, Phys. Rev. B **52**, 14 664 (1995).

<sup>15</sup>A. Franceschetti and A. Zunger (unpublished).

<sup>16</sup>The  $\mathbf{k}_0$  wave vectors of the  $X_{1c}$  valleys are located along the  $\Gamma - X$  lines of the Brillouin zone at a distance  $0.855(2\pi/a)$  from the zone center.